INVITED ARTICLE

Ceramics and amorphous thin films based on gallium sulphide doped by rare-earth sulphides

IOP Publishing Semiconductor Science and Technology
Semicond. Sci. Technol. **30** (2015) 044001 (8pp) doi:10.1088/0268-1242/30/4/044001

Invited Article

Ceramics and amorphous thin films based on gallium sulphide doped by rare-earth sulphides

M Popescu[1], F Sava[1], A Lőrinczi[1], A Velea[1], I D Simandan[1], P Badica[1], M Burdusel[1], A C Galca[1], E Matei[1], N Preda[1], M Secu[1], G Socol[2], F Jipa[2], M Zamfirescu[2] and A Balan[3]

[1] National Institute of Materials Physics, Atomistilor 105bis, RO-077125, PO Box M.G. 7, Magurele-Ilfov, Romania
[2] National Institute for Laser, Plasma and Radiation Physics, Atomistilor 409, RO-077125, PO Box M.G. 36, Magurele-Ilfov, Romania
[3] University of Bucharest, Faculty of Physics, Atomistilor 405, RO-077125, PO Box M.G. 11, 3Nano-SAE Research Centre, Magurele- Ilfov, Romania

E-mail: mihaip58@yahoo.com

Received 12 June 2014, revised 16 October 2014
Accepted for publication 22 October 2014
Published 5 March 2015

Abstract

Bulk ceramics of Ga_2S_3 and rare-earth sulfides (EuS, Gd_2S_3, Er_2S_3) as well as combinations thereof have been prepared by spark plasma sintering (SPS). The disk-shaped ceramics were used as targets for pulsed laser deposition (PLD) experiments to obtain amorphous thin films. The properties of these new bulks and amorphous thin films have been investigated by x-ray diffraction (XRD), scanning electron microscopy (SEM), energy dispersive x-ray spectroscopy (EDX), optical transmission spectroscopy, and atomic force microscopy (AFM). In order to test the photoexpansion effect in Ga_2S_3 and the possibility to create planar arrays of microlenses, the film was irradiated with femtosecond laser pulses at different powers. For low laser power pulses (up to 100 mW power per pulse) a photoexpansion effect was observed, which leads to formation of hillocks with a height of 40–50 nm. EuS doped Ga_2S_3 thin film shows luminescence properties, which recommend them for optoelectronic applications.

Keywords: gallium sulfide, rare-earth sulfides, ceramics, amorphous films, chalcogenide

(Some figures may appear in colour only in the online journal)

1. Introduction

Chalcogenide glasses based on Ga_2S_3 have very attractive properties for a wide range of optical applications [1] such as near- and mid-infrared lasers [2–4], fiber-optic amplifiers [5–7] and acousto-optic devices [8]. They can be drawn into optical fibers [9–13], can form waveguides [14] or can be doped with high concentrations of rare-earth ions [15, 16]. Usually, gallium sulfide glasses are dark yellow or red-brown glasses. Gallium sulfide has a tetrahedrally coordinated layer structure built up from X-M-M-X layers, where M-M are the metal ions sandwiched between chalcogenide atoms (X) [17].

Gallium sulfide chalcogenide glasses are wide-band-gap (around 3.6 eV) semiconductors, making them promising candidates for photovoltaics and optoelectronics if allied with copper and indium [18]. They fill the gap between oxide glasses and indium glasses by showing strong photo-luminescent emissions that can be varied in the range of

a. b. c. d.

Figure 1. The image of sintered disks using spark plasma sintering: (a) Ga_2S_3, (b) Ga_2S_3:EuS, (c) Ga_2S_3: Er_2S_3, (d) Ga_2S_3:Gd_2S_3.

470–520 nm [19]. When doped with rare-earth ions and irradiated with an appropriate wavelength, they exhibit fluorescence and can be used as amplifiers in the infrared region [20].

Gallium sulfide based glasses possess a very high rare-earth solubility, excellent UV edge and low fibre attenuation in the near infrared range [21].

The most known rare-earth doped gallium sulfide glasses are the gallium–lanthanum-sulfides which have been proposed as rare-earth hosts for 1.3 μm optical amplification devices [22].

The regular techniques for obtaining gallium sulfide thin films do not typically provide the necessary control over thickness and stoichiometry required for the precise synthesis of nanostructured materials. On the other hand, it is not an easy task to obtain completely amorphous rare-earth doped gallium sulfide thin films.

In this paper we report the successful preparation of amorphous gallium sulfide thin films doped by rare-earth sulfides by using pulsed laser deposition technique. The optical and photoluminescence properties of these films make them good candidates for applications in optoelectronic circuits.

2. Materials and methods

In order to check if gallium sulfide is a good host for accommodating rare-earth ions, we have prepared Ga_2S_3 disc-shaped bulk ceramics doped with 5% EuS, 5% Er_2S_3 and 5% Gd_2S_3 (figures 1(a)–(d)) using spark plasma sintering (SPS). The last two samples (figures 1(c), (d)) have cracked due to the stress accumulated in them during cooling. For comparison, additional bulk samples of EuS, Er_2S_3 and Gd_2S_3 disc-shape have been prepared using the same technique.

Ga_2S_3 (with a small amount of Ga_2O_3) and high purity rare-earth sulfide (99.99%) powders purchased from Alpha-AESAR and CHEMOS GmbH were used to prepare mixtures with the starting compositions of $(Ga_2S_3)_{0.95}(ReS_x)_{0.05}$ at. %, (where ReS_x = EuS, Er_2S_3 and Gd_2S_3). The mixtures were prepared under ambient conditions by mecanical grinding for 360 s in an agate mortar and then they were used for SPS consolidation.

Spark plasma sintering simultaneously applies a pulsed current and a uniaxial pressure on punches of a mould system that is loaded with powder. SPS has several unique and specific features. The use of pulsed currents during SPS induces unconventional features leading to activated sintering. Literature indicates formation of 'hot spots', enhanced electro-diffusion and surface/boundary cleaning, occurrence of controversial spark or spark plasma effects, and heating from inside to outside as for microwave sintering [23–28]. Among the consequences are high efficiency of sintering toward high density bulks, often for lower processing times and temperatures. SPS is more flexible than common high-temperature hot pressing. For example, SPS allows high heating/cooling rates useful to avoid excessive coarsening of grains. All these features generate morphologies that are not observed when using conventional sintering methods. The powders (3.4 g) were wrapped into C-paper, loaded into a 2 cm inner diameter graphite die and processed by spark plasma sintering (SPS) at 900 °C for 5 min. The heating rate was 100 °C min^{-1} while the uniaxial pressure applied on punches was 60 MPa. The initial vacuum in the SPS furnace was 40 Pa. The temperature was measured using a thermocouple located at 2 mm from the sample and introduced through a hole made in the mould. A pulsed current pattern of 12-on/2-off pulses was applied, with a 3 ms period. The total time of one sequence was ~0.04 s. The operating voltage and the peak current were up to 5 V and 1600 A, respectively. We used a commercial SPS machine FCT Systeme GmbH—HP D 5, Germany.

The sintered ceramic disks of 2 cm in diameter have been used as targets for pulsed laser deposition (PLD) of thin films. PLD is known to be a technique which preserves the stoichiometry of the target in thin films while the thickness of the films can be easily controlled. The depositions were performed in a stainless steel chamber using a KrF* laser source, model COMPexPro 205, Lambda Physics-Coherent (λ = 248 nm, τ_{FWHM} = 25 ns) that operated at a repetition rate of 10 Hz. The targets were irradiated at a laser fluence of 3 J cm^{-2} while a target-substrate separation distance of 5 cm was chosen. Before the deposition experiment, the reaction chamber was evacuated to a residual pressure of 5×10^{-4} Pa. During the laser ablation process, the glass substrates were kept at room temperature and continuously rotated in order to improve their thickness uniformity. Prior to introduction inside the deposition chamber, the substrates were successively cleaned into an ultrasonic bath with acetone, ethanol and deionized water for 15 min.

All the bulk samples and the thin films have been studied by x-ray diffraction (XRD), scanning electron microscopy (SEM), energy dispersive x-ray spectroscopy (EDX), optical transmission spectroscopy and atomic force microscopy (AFM).

The x-ray diffraction curves of thin films have been carried out with Bruker A8 Advanced provided with CuK_α target tube, scintillation counter, Göbell mirror and asymmetric channel-cut (ACC) Ge (220) to get a parallel monochromatic beam. The incidence angle was fixed at 0.6°, while the detector has been moved with an angular step of 0.05° (2θ). The counting time per step was of 64 s.

For producing microstructures (hillocks or hole) on Ga_2S_3 thin film a standard laser micro-processing setup was used. The laser source was a femtosecond oscillator Synergy Pro with 800 nm central wavelength, 15 fs pulse duration, 80 MHz repetition rate, and 5 nJ maximum energy per pulse.

The microprocessing setup is equipped with a dispersion compensation module and a spatial filter to preserve a good spatial profile and very short pulse duration. Thus, after filtering, the laser beam has a Gaussian spatial profile with beam diameter of 3 mm at $1/e^2$. A NIR Mitutoyo microscope objective with 0.5 numerical apertures and 100x magnification was used to focus the laser beam. The estimated diameter spot in the focal plane is 3 μm. The size of the microstructures produced by laser irradiation on the sample is given by the laser intensity and the exposure time. The laser power is controlled using a half-wave plate and two polarizers in reflection to minimise the temporal dispersion. The sample is shifted along XY directions using a translation stage with maxim travel range of 50 mm on each axis. The irradiation was performed for 300 ms at each point. The laser power was varied from 20 to 120 mW. For one value of laser power, a network of microstructures with periodicity of 5 μm is created. Not only the size but also the shape of the produced features is found to dramatically change with the laser power.

Atomic force microscopy (AFM) topography images were obtained by means of SPM-NTegra Prima AFM (NT-MDT), operated in semicontact mode, using an NSG 01 cantilever (resonance frequency: 83–230 kHz, elastic constant: 1.45–15.1 N m^{-1}), scan rate 1 Hz. Images were obtained by displaying the height signal acquired in forward direction at 256 × 256 pixels image resolution.

The optical transmission measurements have been performed by using a spectrophotometer UV–vis-NIR Cary 5000.

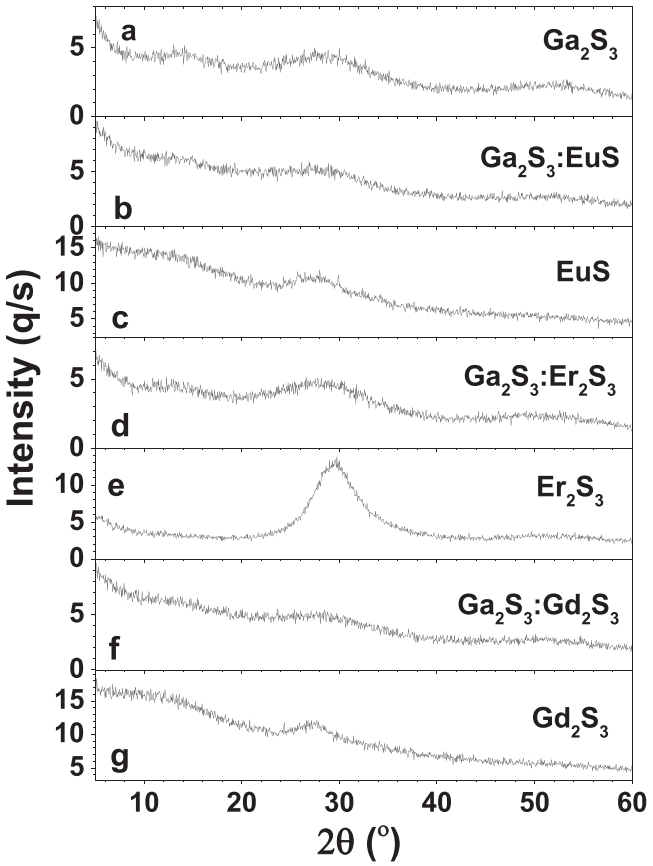

Figure 2. X-ray diffraction diagrams of the investigated amorphous thin films.

3. Results and discussion

3.1. Structural properties of bulk ceramics

The resulting ceramics based on undoped and doped Ga_2S_3 are polycrystalline and they contain small amounts of base-centered monoclinic Ga_2O_3. The structure of ceramic Ga_2S_3 is base-centered monoclinic. The doped ceramics Ga_2S_3 contain, besides the base-centered monoclinic Ga_2S_3, ternary compounds such as face-centered orthorhombic $EuGa_2S_4$ in Ga_2S_3:EuS or base-centered orthorhombic Er_3GaS_6 in Ga_2S_3:Er_2S_3. The rare-earth sulfides are also polycrystalline in the ceramic disks and they have the following symmetries: face-centered cubic for EuS, monoclinic for Er_2S_3 and orthorhombic for Gd_2S_3. The XRD data on the ceramics bulk are not shown.

The mass density (ρ) and microhardness on Vickers scale (HV) of the ceramics are presented in the table 1. The obtained disks are compact and their density approaches that of crystalline phase.

The mass density of the hexagonal Ga_2S_3 is 3.77 g cm^{-3} [29].

Table 1. The microhardness on Vickers scale (HV) and mass density (ρ) of the ceramics samples.

	HV (kgF mm^{-2})	ρ(g cm^{-3})
bulk Ga_2S_3	183.89	3.49
bulk Ga_2S_3:Eu_2S_3	204.13	3.81
bulk Ga_2S_3:Er_2S_3	196.78	3.72
bulk Ga_2S_3:Gd_2S_3	251.04	3.74

3.2. Structural properties of thin films

The x-ray diffraction patterns of the thin films are presented in figure 2. All the PLD prepared films are amorphous with an approximate thickness of 1.7 μm for Ga_2S_3 undoped and doped with rare-earth sulfides, 2.35 μm for EuS, 3.3 μm for Gd_2S_3 and 2.9 μm for Er_2S_3. This result is remarkable and PLD proved to be a convenient technique for obtaining completely amorphous thin films.

From EDX data we have obtained that the concentration of sulphur in the thin films is lower than in the corresponding bulk samples. Thus, in fact the Ga_2S_3 sample has the formula $Ga_2S_{2.27}O_{0.73}$, EuS is $Eu_{3.12}S_{1.88}$, Er_2S_3 is $Er_{3.46}S_{1.54}$ and Gd_2S_3 is $Gd_{3.05}S_{1.95}$.

In figures 2(a), (b), (d), (f) can be observed in the first part of x-ray diagrams of the amorphous thin films a first sharp diffraction peak (FSDP) similar to that observed in As_2S_3 amorphous thin films [30]. The structure of Ga_2S_3 amorphous thin films (undoped or doped with rare-earth sulfides) can be considered as a packing of disordered layers, as in As_2S_3 amorphous thin films [31]. Thus, the features of

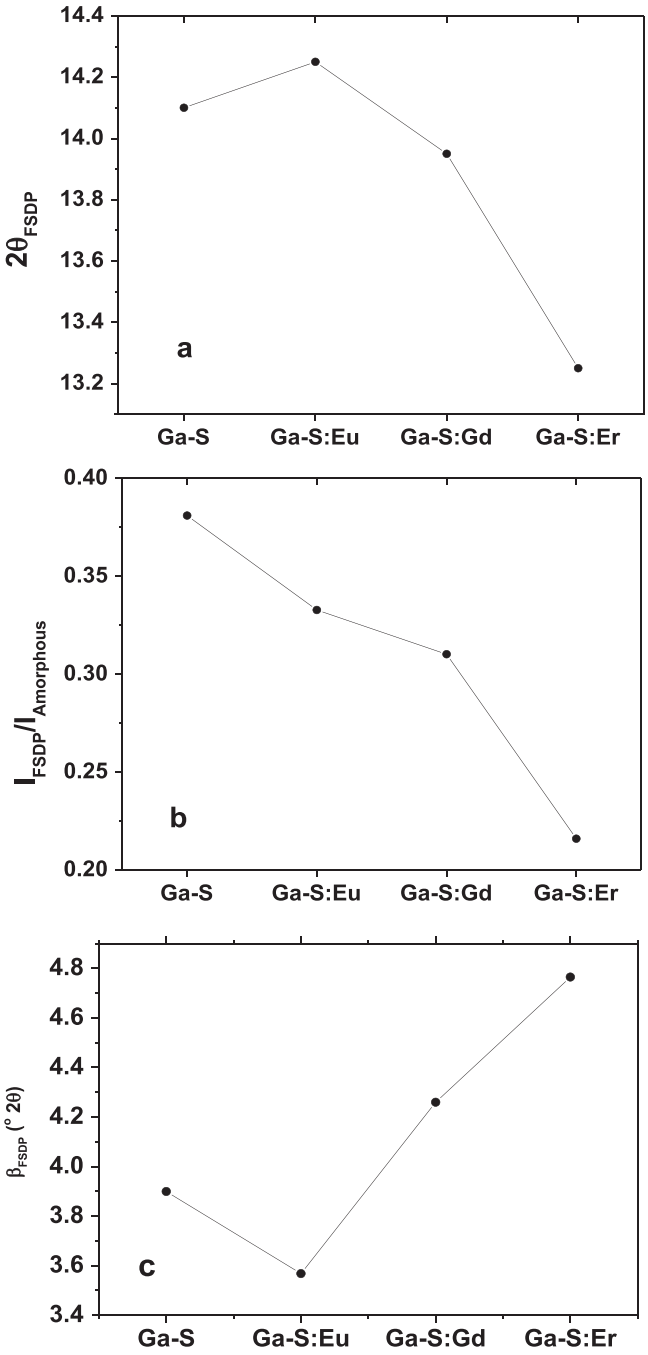

Figure 3. The parameters of FSDP as a function of the composition of the thin films: (a) the position of the FSDP ($2\theta_{FSDP}$), (b) the ratio of the x-ray intensity of the FSDP (I_{FSDP}) to the x-ray intensity of the next maximum ($I_{amorphous}$), (c) full width at half maximum (β_{FSDP}).

FSDP peak can be used to characterize (on average) the domains with a more orderly packing of amorphous layers. Work is in progress for modelling the amorphous Ga_2S_3 structure. The characterization of this FSDP for our samples is given in figures 3(a)–(c).

From figure 3(a) results that the interlayer distance is the smallest for Ga_2S_3:EuS and the highest for Ga_2S_3:Er_2S_3 while figures 3(b), (c) show that layer disorder decreased from Ga_2S_3:EuS to Ga_2S_3:Er_2S_3. This effect is due to the increase of radius of RE dopants.

3.3. SEM images of ceramic disks prepared by SPS

SEM images of the surfaces and cross sections of the ceramic disks are shown in figures 4(b)–(g). A compact material exhibiting grains of several micrometers in size and inhomogeneous morphologies can be observed. For comparison the morphology of the Ga_2S_3 powder is presented in figure 4(a).

The electron micrographs of the amorphous thin films do not show any evidence of recognizable structure (data not shown).

3.4. Optical properties

The optical transmission curves for the amorphous thin films were measured in the range of 200–800 nm and are shown in figure 5 together with optical absorption edges and optical band gaps.

The optical band gap for the prepared sulfide amorphous thin films was obtained using the plot $(I_{Abs})^{1/2} = f[E(\text{eV})]$, where E(eV) is the energy of light quanta expressed in electronvolts and $I_{Abs} = \ln(100/I_T)$, $I_T = f(E(\text{eV}))$ is the optical transmission curve.

A linear correlation between optical band gap and the molecular weight of the thin films is observed in figure 6.

Photoluminescence spectra recorded on undoped and EuS doped Ga_2S_3 bulk polycrystalline samples are presented in figures 7(a), (b). The undoped Ga_2S_3 bulk sample shows a relatively weak and broad peak at about 430 nm, while in the case of EuS doped bulk sample a new broad and strong peak emerges at about 537 nm that was ascribed to the $4f^6 5d \rightarrow {}^8S_{7/2}$ transition of Eu^{2+} dopant ions.

The very similar shape and intensity in the cases of EuS doped Ga_2S_3 (figure 7(c)) and EuS (figure 7(d)) amorphous thin films are probably due to the similar cluster formation of the EuS dopant. The peak at 492.9 nm seems to correspond to transition $4f^6 5d^1 \rightarrow 4f^7$ of Eu^{2+} ions. It was not possible to measure the luminescence of Er doped Ga_2S_3 and Gd doped Ga_2S_3.

From the ellipsometric measurements we inferred the refractive index of Ga_2S_3, EuS, Er_2S_3 and Gd_2S_3 amorphous thin films (figure 8). It is remarkable that the refractive index of Ga_2S_3 is 2.95 at $\lambda = 400$ nm.

The optical properties of the rare-earth doped gallium sulfide thin films make them promising candidates for planar waveguides and light polarizer applications.

3.5. Photoexpansion effect and microlens formation in Ga_2S_3 amorphous thin films

Thin amorphous films of Ga_2S_3 have been irradiated with femtosecond laser pulses at the wavelength of 800 nm.

Figures 9(a)–(g) show the AFM images of the irradiated films.

In the case of the irradiation with low laser power pulses (between 85 and 100 mW power per pulse), a photoexpansion effect was observed that results in the formation of the hillocks (figures 9(a)–(d)) with a height of 40–50 nm due to the increase of volume with ~2.46%, a similar phenomenon to that which has been also observed in our amorphous As_2S_3 films [32].

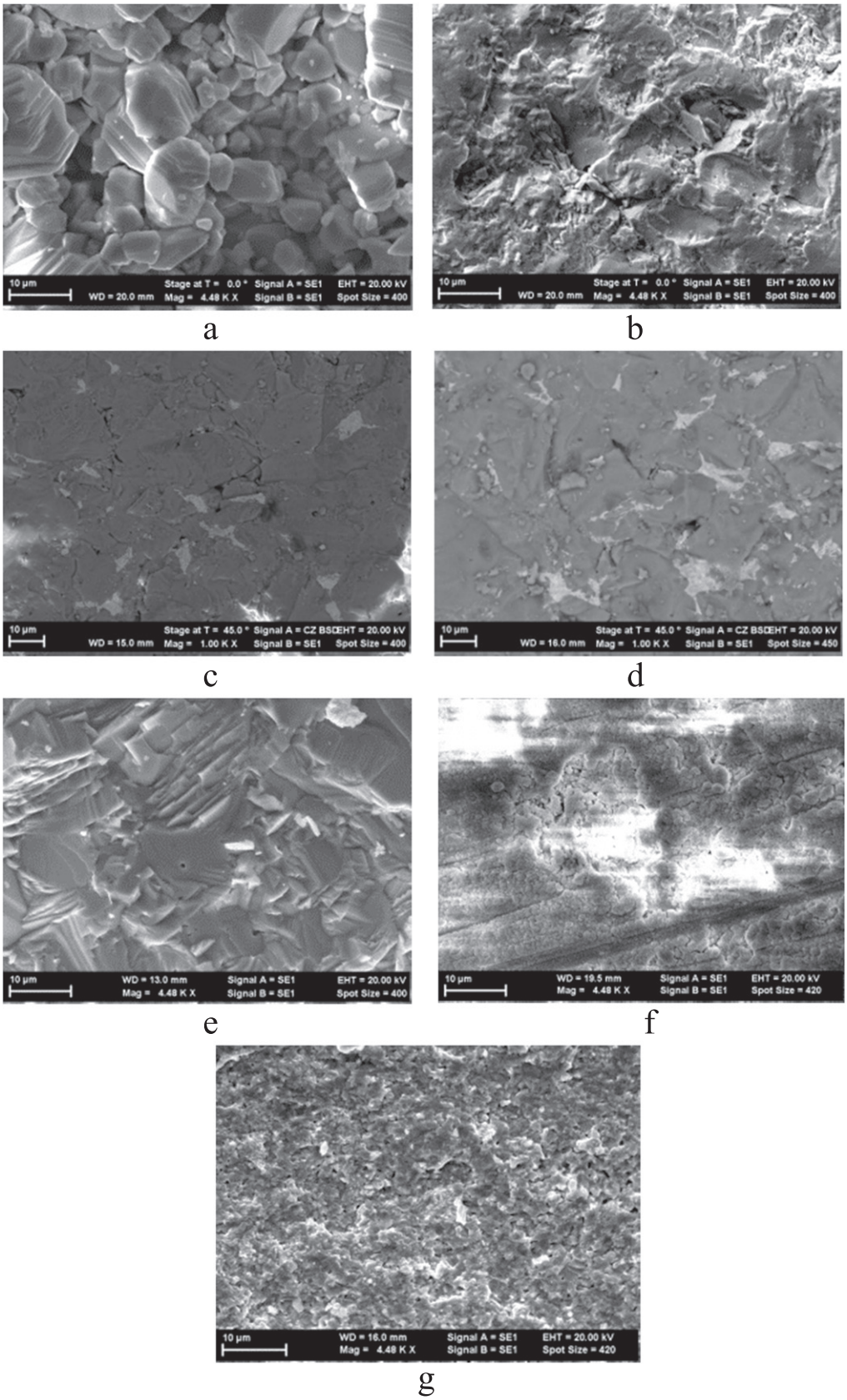

Figure 4. Typical SEM micrographs of (a) Ga_2S_3 powder, (b) surface of Ga_2S_3 ceramic bulk, (c) cross section of Ga_2S_3:Er_2S_3 ceramic bulk, (d) cross section of Ga_2S_3:Gd_2S_3 ceramic bulk, (e) cross section of EuS ceramic bulk, (f) surface of Er_2S_3 ceramic bulk, (g) cross section of Gd_2S_3 ceramic bulk. (Ga_2S_3:EuS is not shown because of the electrical charging of the sample).

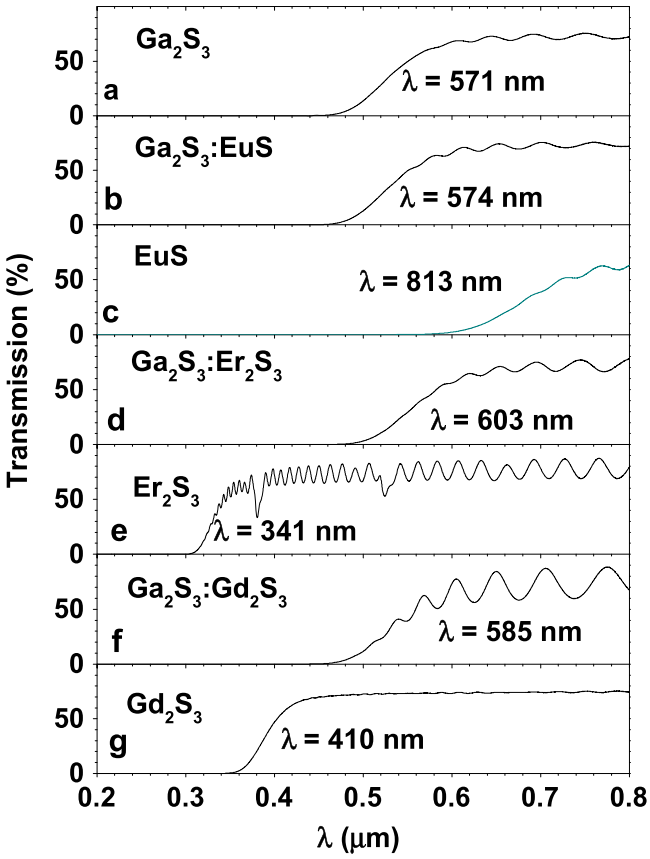

Figure 5. The optical transmission spectra and optical absorption edge of the investigated amorphous thin films. The inferred optical band gaps are: (a) 2.17 eV, (b) 2.16 eV, (c) 1.52 eV, (d) 2.06 eV, (e) 3.64 eV, (f) 2.12 eV, (g) 3.02 eV.

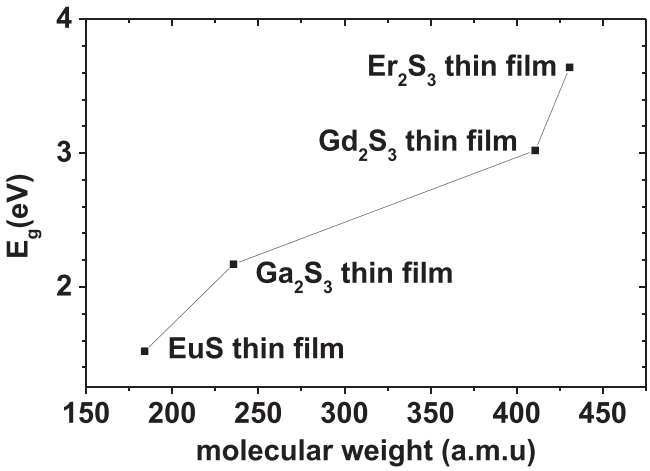

Figure 6. The plot of optical band gaps versus molecular weight of the main thin films.

For large power pulses (higher than 105 mW power per pulse) the laser beam induces holes (figures 9(e)–(g)) in the center of the irradiated area. Both processes occur at higher powers of pulses than those used in the case of As_2S_3 amorphous thin films [32].

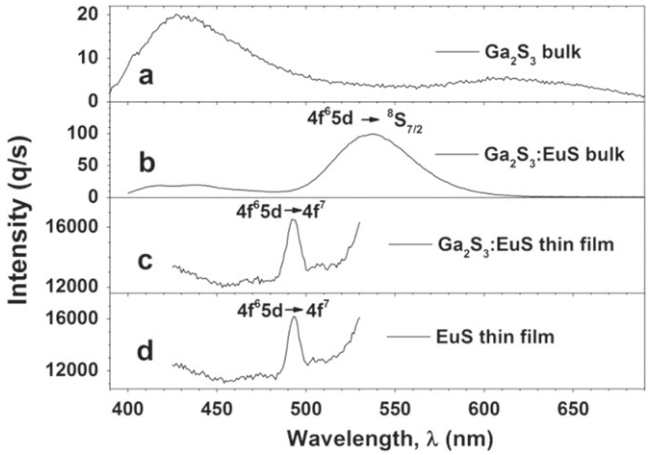

Figure 7. Luminescence measurements on (a) Ga_2S_3 and (b) Ga_2S_3:EuS bulk samples (using an excitation radiation with $\lambda = 350$ nm), (c) Ga_2S_3:EuS and (d) EuS amorphous thin films (using an excitation radiation with $\lambda = 300$ nm).

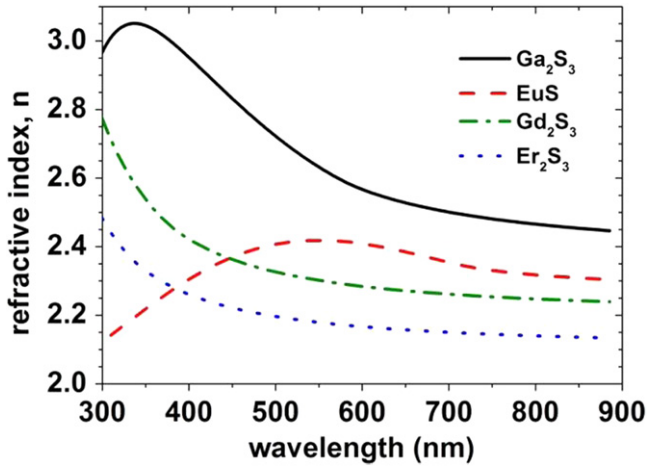

Figure 8. The refractive index (n) of amorphous thin films of Ga_2S_3, EuS, Er_2S_3 and Gd_2S_3.

4. Conclusions

New ceramics and amorphous thin films based on Ga_2S_3 and rare-earth sulfides have been successfully prepared by SPS and PLD. The SPS method ensures a high density and good mechanical properties of the sinter gallium sulfide based ceramics.

Photoluminescence properties have been observed in both bulk samples and amorphous thin films.

The refractive index of Ga_2S_3 films inferred by spectroscopic ellipsometry was of 2.95 at $\lambda = 400$ nm, which ensures their applications in optoelectronic devices.

Femtosecond laser irradiation experiments evidenced a photoexpansion effect in Ga_2S_3 thin films similar to that found in As_2S_3 films.

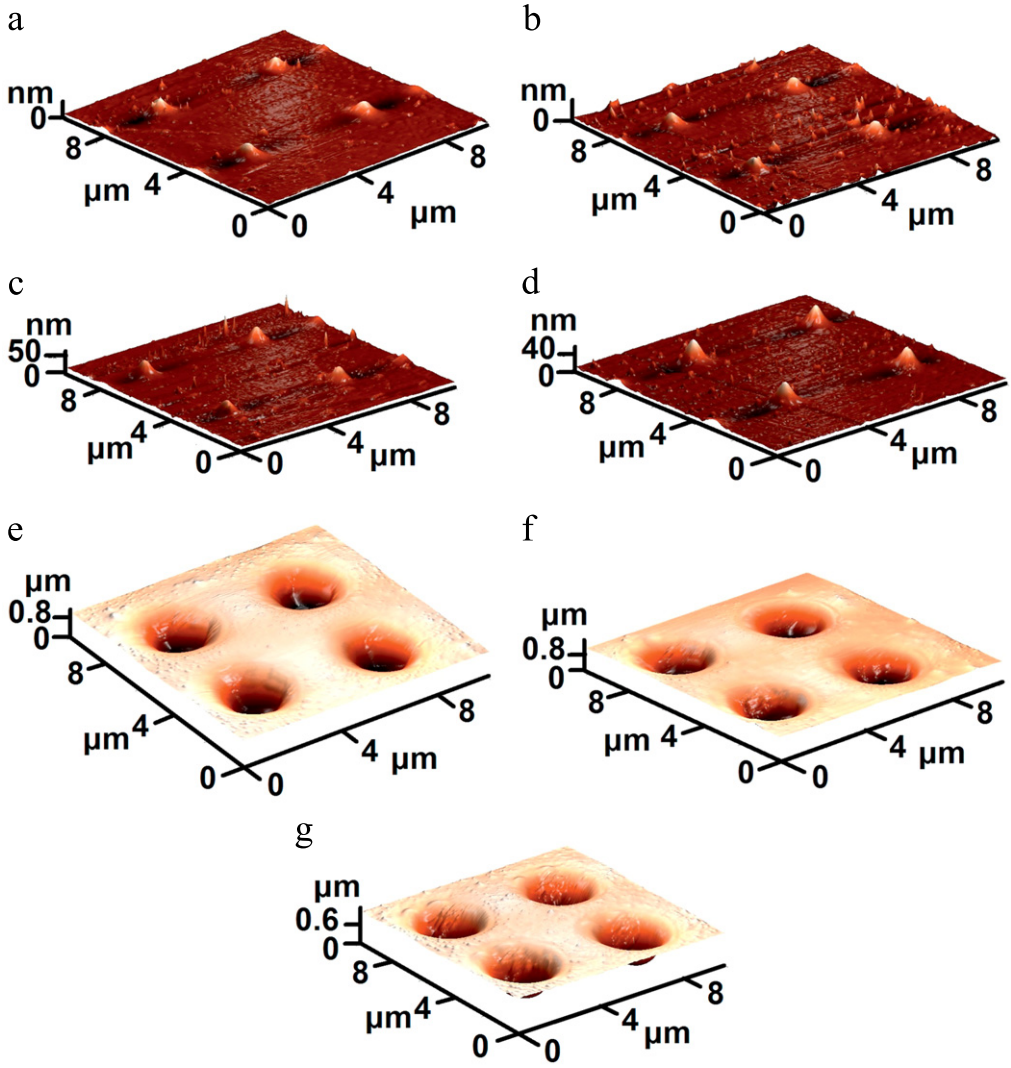

Figure 9. The AFM images of Ga_2S_3 thin films irradiated at different powers of the femtosecond laser pulses: (a) P = 85 mW, (b) P = 90 mW, (c) P = 95 mW, (d) P = 100 mW, (e) P = 105 mW, (f) P = 115 mW, (g) P = 120 mW.

Acknowledgments

The authors acknowledge the financial support of the Ministry of National Education (Romania) in the frame of the Project PN45N 2009.

References

[1] Kumta P N and Risbud S H 1994 *J. Mater. Sci.* **29** 1135
[2] Schweizer T, Samson B N, Moore R C, Hewak D W and Payne D N 1997 *Electron. Lett.* **33** 414
[3] Schweizer T, Brady D J and Hewak D W 1997 *Opt. Express* **1** 102
[4] Schweizer T, Samson B N, Hector J R, Brocklesby W S, Hewak D W and Payne D N 1999 *J. Opt. Soc. Am.* B **16** 308
[5] Tawarayama H, Ishikawa E, Yamanaka K, Itoh K, Okada K, Aoki H, Yanagita H, Matsuoka Y and Toratani H 2000 *J. Am. Ceram. Soc.* **83** 792
[6] Li R, Furniss D, Bagshaw H and Seddon A B 1999 *J. Mater. Res.* **14** 2621
[7] Wang J, Hector J R, Brady D, Hewak D, Brocklesby B, Kluth M, Moore R and Payne D N 1997 *Appl. Phys. Lett.* **71** 1753
[8] Abdulhalim I, Pannell C N, Deol R S, Hewak D W, Wylangowski G and Payne D N 1993 *J. Non-Cryst. Solids* **164–166** 1251
[9] Hewak D W, Moore R C, Schweizer T, Wang J, Samson B, Brocklesby W S, Payne D N and Tarbox E J 1996 *Electron. Lett.* **32** 384
[10] Furniss D and Seddon A B 1999 *J. Non-Cryst. Solids* **256–257** 232
[11] West Y D, Schweizer T, Brady D J and Hewak D W 2000 *Fiber Integr. Opt.* **19** 229
[12] Monro T M, West Y D, Hewak D W, Broderick N G R and Richardson D J 2000 *Electron. Lett.* **36** 1998
[13] Sanghera J S *et al* 2000 *Fiber Integr. Opt.* **19** 251
[14] Mairaj A K, Hua P, Rutt H N and Hewak D W 2002 *J. Lightwave Technol.* **20** 1578
[15] Loireau-Lozac'h A-M, Guittard M and Flahaut J 1976 *Mater. Res. Bull.* **11** 1489
[16] Takebe H, Ishibashi T, Ichiki T and Morinaga K 2003 *J. Ceram. Soc. Japan* **111** 755
[17] Al-Alamy F A S and Balchin A A 1977 *J. Cryst. Growth* **39** 275–86

[18] Vasekar P S, Jahagirdar A H and Dhere N G 2010 *Thin Solid Films* **518** 1788–90
[19] Zheng N, Bu X and Feng P 2003 *J. Am. Chem. Soc.* **125** 1138
[20] Machewirt D P, Wei K, Krasteva V, Datta R, Snitzer E and Sigel G H 1997 *J. Non-Cryst. Solids* **213** 295
[21] Kobelke J, Jetschke S, Schwuchow A, Kirchhof J and Schuster K 2003 *J. Non-Cryst. Solids* **326&327** 446
[22] Li R and Seddon A B 1999 *J. Non-Cryst. Solids* **256–257** 17
[23] Munir Z A, Anselmi-Tamburini U and Ohyanagi M 2006 *J. Mater. Sci.* **41** 763
[24] Risbud S H, Groza J R and Kim M J 1994 *Philos. Mag.* B **69** 525
[25] Groza J R and Zavaliangos A 2000 *Mater. Sci. Eng.* A **287** 171
[26] Chaim R, Levin M, Slayer A and Estournes C 2008 *Adv. Appl. Ceram.* **107** 159
[27] Badica P, Crisan A, Aldica G, Endo K, Borodianska H, Togano K, Awaji S, Watanabe K, Sakka Y and Vasylkiv O 2011 *Sci. Technol. Adv. Mater.* **12** 013001
[28] Demirskyi D, Borodianska H, Agrawal D, Ragulya A, Sakka Y and Vasylkiv O 2012 *J. Alloys Compd.* **523** 1
[29] Dale L P 2011 *Handbook of Inorganic Compounds* 2nd ed (New York: CRC Press)
[30] Georgescu G, Sava F and Rares-Medianu M 2006 *J. Optoelectron. Adv. Mater.* **8** 1801
[31] Lőrinczi A and Sava F 2005 *Chalcogenide Lett.* **2** 1
[32] Velea A *et al* 2012 *J. Appl. Phys.* **112** 033105–033101